Supporting Information

The efficacy of Pb, As(V) and Sb(III) removal by biochar is determined by solution chemistry

Sampriti Chaudhuri[a,b], Gabriel Sigmund[a,c*], Naresh Kumar[d], Thorsten Hüffer[a], Andreas Mautner[e,f], Thilo Hofmann[a*]

[a] Department of Environmental Geosciences, Centre for Microbiology and Environmental Systems Science, University of Vienna, Josef-Holaubek Platz 2, 1090 Vienna, Austria

[b] Doctoral School in Microbiology and Environmental Science, University of Vienna, 1090 Vienna, Austria

[c] Environmental Technology, Wageningen University, P.O. Box 17, 6700 AA Wageningen, The Netherlands

[d] Soil Chemistry, Wageningen University, 6708 PB Wageningen, The Netherlands

[e] Institute of Materials Chemistry and Research, Polymer and Composite Engineering (PaCE) Group, Faculty of Chemistry, University of Vienna, Währinger Strasse 42, 1090, Vienna, Austria

[f] Institute of Environmental Biotechnology, IFA-Tulln, University of Natural Resources & Life Sciences (BOKU), Konrad-Lorenz-Straße 20, 3430, Tulln an der Donau, Austria

ORCID:

SC: 0000-0002-8693-8758

GS: 0000-0003-2068-0878

NK: 0000-0002-8593-5758

THü: 0000-0002-5639-8789

AM: 0000-0003-0347-8643

THo: 0000-0001-8929-6933

Corresponding authors:

Gabriel Sigmund, Department of Environmental Geosciences, Centre for Microbiology and Environmental Systems Science, University of Vienna, Josef-Holaubek Platz 2, 1090 Vienna, Austria and Environmental Technology, Wageningen University, P.O. Box 17, 6700 AA Wageningen, The Netherlands; Email: gabriel.sigmund@wur.nl

Thilo Hofmann, Department of Environmental Geosciences, Centre for Microbiology and Environmental Systems Science, University of Vienna, Josef-Holaubek Platz 2, 1090 Vienna, Austria; Email: thilo.hofmann@univie.ac.at

1. Central Composite Design

Table S1: Design matrix used in sorption experiments

	Runs	Ca	P	DOC	Fe
cube points	1	low	low	low	low
	2	high	low	low	low
	3	low	high	low	low
	4	high	high	low	low
	5	low	low	high	low
	6	high	low	high	low
	7	low	high	high	low
	8	high	high	high	low
	9	low	low	low	high
	10	high	low	low	high
	11	low	high	low	high
	12	high	high	low	high
	13	low	low	high	high
	14	high	low	high	high
	15	low	high	high	high
	16	high	high	high	high
central points	17	medium	medium	medium	medium
	18	medium	medium	medium	medium
	19	medium	medium	medium	medium
	20	medium	medium	medium	medium
	21	medium	medium	medium	medium
	22	medium	medium	medium	medium
	23	medium	medium	medium	medium
axial points	24	very low	medium	medium	medium
	25	very high	medium	medium	medium
	26	medium	very low	medium	medium
	27	medium	very high	medium	medium
	28	medium	medium	very low	medium
	29	medium	medium	very high	medium
	30	medium	medium	medium	very low
	31	medium	medium	medium	very high

Very low, low, medium, high, very high correspond to the –α, −1, 0, +1, +α values provided in Table 1 of the main text.

2. Selection of BCs

Sorbent screening tests were conducted in preliminary experiments to choose an optimal sorbent for each of the metal(loid)s. Sorption experiments were done at a solid:liquid ratio of 1:1000 in ultrapure water using the 12 BC listed in Table S2. After adding 10 mg of BC and 10 mL ultrapure water in a 15 mL polystyrene tube, the suspension was allowed to equilibrate for two hours, after which the metal(loid)s were spiked at a concentration of 1 mg L^{-1}.

Table S2: List of materials screened for suitability of metal(loid) sorption

BC	FEEDSTOCK	PYROLYSIS TEMP.	MANUFACTURER
SWP550	Soft wood pellets	550ºC	UK Biochar Research Centre, UK
SWP700	Soft wood pellets	700ºC	UK Biochar Research Centre, UK
WSP550	Wheat straw pellets	550ºC	UK Biochar Research Centre, UK
WSP700	Wheat straw pellets	700ºC	UK Biochar Research Centre, UK
RH550	Rice husk	550ºC	UK Biochar Research Centre, UK
RH700	Rice husk	700ºC	UK Biochar Research Centre, UK
MSP550	Miscanthus straw pellets	550ºC	UK Biochar Research Centre, UK
MSP700	Miscanthus straw pellets	700ºC	UK Biochar Research Centre, UK
OSR550	Oil seed rape	550ºC	UK Biochar Research Centre, UK
ORS700	Oil seed rape	700ºC	UK Biochar Research Centre, UK
SAWC	Steam activated wood char	900ºC	Ithaka Institute, Switzerland
BCD	Wood biomass-dolomite blend	850ºC	University of Bologna, Italy

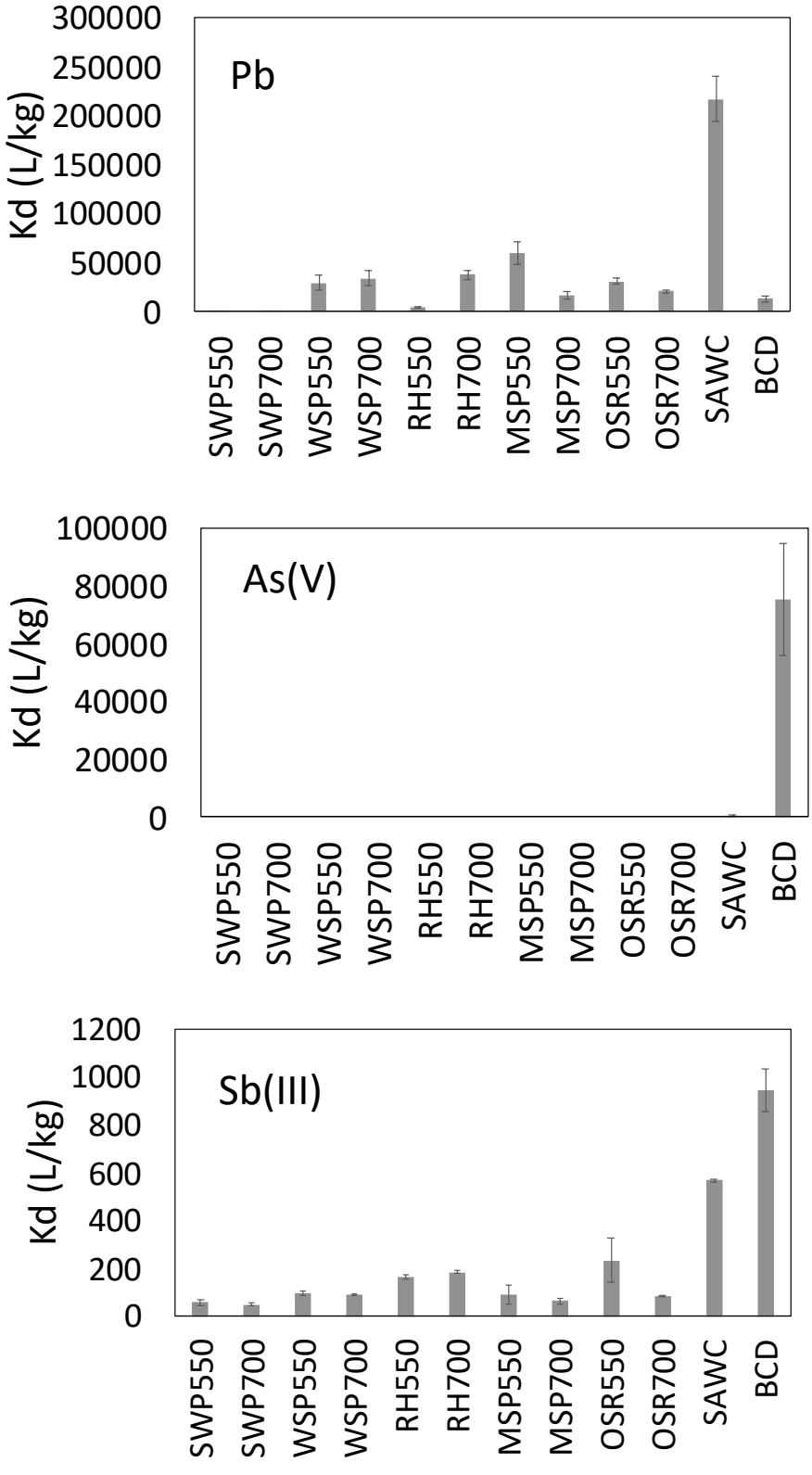

Figure S1. Sorption coefficients of Pb, As(V), and Sb(III) with different BCs during screening tests in ultrapure water. SAWC and MSP550 removed Pb most efficiently out of all sorbents. Only BCD was able to remove As(V). BCD and SAWC were able to remove Sb(III). In order to investigate a different sorbent for each of the metal(loid)s,

we selected MSP550 for Pb, BCD for As(V), and SAWC for Sb(III). In this way we could include an un-activated biochar, a biochar-dolomite composite, and a steam-activated biochar in the study.

3. Calculation of sorption coefficients and removal

The amount of metal(loid)s immobilized by BCs, the equilibrium sorption coefficients and the % removal of metal(loid)s were calculated using the following equations:

Equilibrium sorption coefficients	**Surface area normalized equilibrium sorption coefficient**	**Removal (%)**
$q_e = \frac{V(C_0 - C_e)}{W}$	$q_{e,SSA} = \frac{V(C_0 - C_e)}{W \times SSA}$	$Removal = \frac{(C_0 - C_e)}{C_0} \times 100$
$K_d = \frac{q_e}{C_e}$	$K_{SSA} = \frac{q_{e,SSA}}{C_e}$	

where q_e (mg kg^{-1}) is the mass of metal(loid) sorbed per unit mass of the BC at equilibrium; $q_{e,SSA}$ (mg m^{-2}) is the mass of metal(loid) sorbed per unit specific surface area of the BC at equilibrium; C_0 and C_e (mg L^{-1}) are the initial and equilibrium metal(loid) concentrations in the aqueous phase respectively; W(kg) is the mass of BC; V(L) is the volume of the aqueous phase; SSA (m^2 kg^{-1}) is the specific surface area of the BC per unit mass; K_d (L kg^{-1}) is the sorbent mass normalized equilibrium sorption coefficient; K_{SSA} is the specific surface area normalized equilibrium sorption coefficient.

4. Sb speciation using HPLC-ICP-MS

The methodology for determining Sb(III)/Sb(V) speciation using HPLC-ICP-MS was adopted from Zheng et al, 2001 (Zheng et al., 2001). Immediately at the end of experiments, samples were stabilized by adding citric acid at a concentration of 26 mM to preserve the redox state of Sb. A stock solution of 10 mg L^{-1} of Sb(III) and Sb(V) for HPLC-ICP-MS was freshly prepared by dissolving $K_2[Sb_2(C_4H_2O_6)_2]\cdot 3H_2O$

and $KSb(OH)_6$ in 26 mM citric acid. Sb(III)/(V) standards for HPLC-ICP-MS were obtained by diluting this stock solution to the required concentrations. A Hamilton PRP X-100 anion exchange separation column (250 mm x 4.6 mm id, 10 mm particle size, Hamilton, USA) was used to separate the two species of Sb. 10 mM of ethylene diamine tetra acetic acid (EDTA) with 1 mM phthalic acid was used as the HPLC mobile phase (flow rate: 1.5 mL min^{-1}; injection volume: 100 µL; pH: 4.5). A flow split was installed before the ICP-MS, and a micro flow meter (TruFlo Sample Monitor 0–4.0 mL min^{-1}, Glass Expansion, Melbourne, Australia) monitored the reduced flow rate (0.4 mL min^{-1}). Effective peak separation and quantification of Sb(V)-citrate was achieved at 10 µg L^{-1}.The limit of quantification for Sb(III)-citrate species was 1 µg L^{-1}.

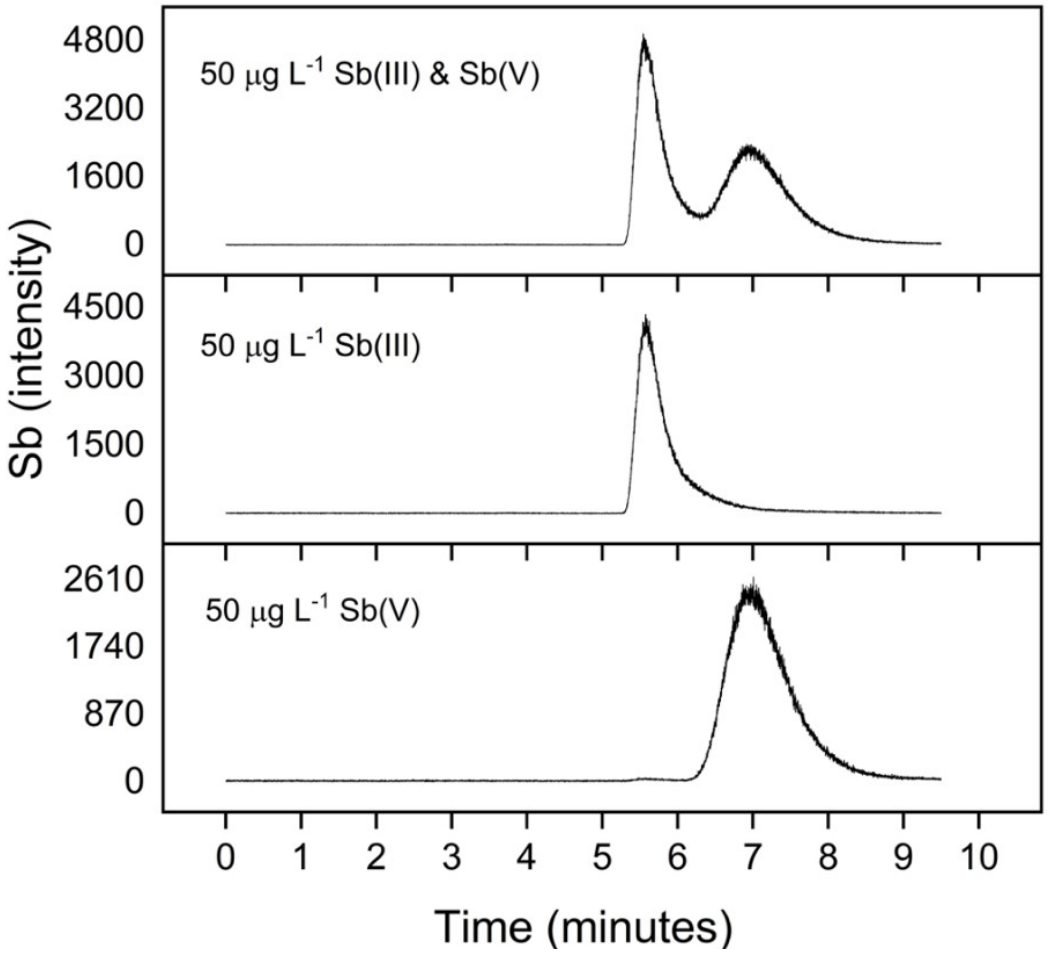

Figure S2. Time resolved chromatograms of 50 µg L^{-1} Sb(III)-citrate and 50 µg L^{-1} Sb(V)-citrate spiked together, 50 µg L^{-1} Sb(III) complexed to citrate, and 50 µg L^{-1} Sb(V) complexed to citrate (top to bottom).

5. Effects of Fe(III) on Sb(III) sorption

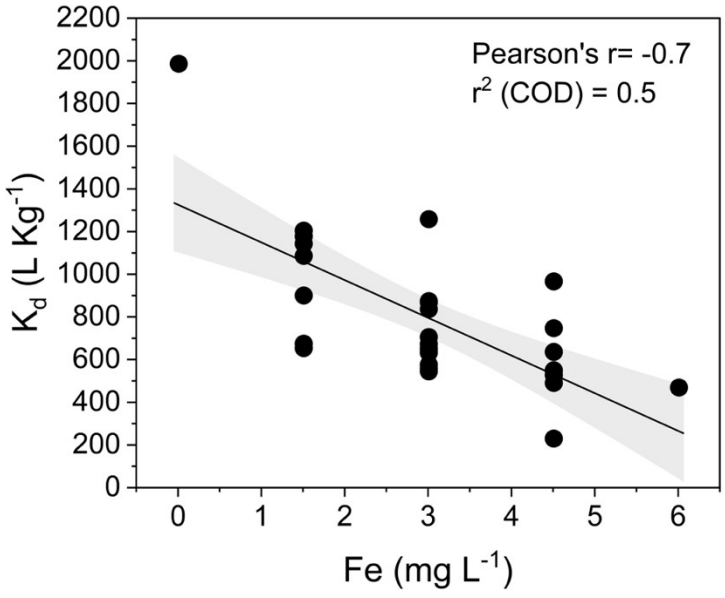

Figure S3. Regression and Pearson's correlation of sorption coefficients (K_d) of Sb(III)-SAWC with added Fe(III). 95% confidence band added.

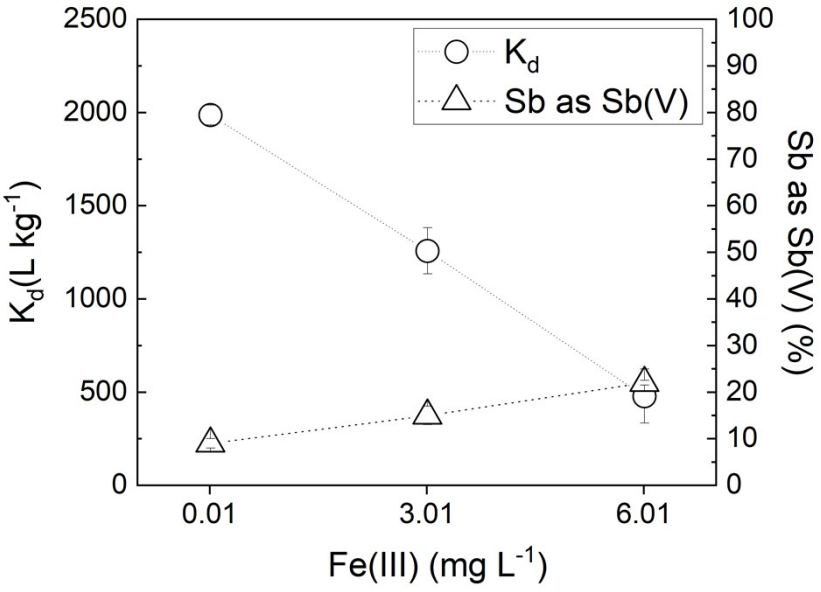

Figure S4. Sorption coefficients for Sb-SAWC across three different added Fe(III) concentrations (bars) in the design matrix. % Sb(V) formed in the aqueous phase without SAWC (controls) at those points in the design matrix.

Table S3: Sb(V) sorption to SAWC

Design points in CCD from **table S1**	Ca^{2+}	P	DOC	Fe(III)	Sb,control	Sb,SAWC
	mg L^{-1}					
Cube point 1	48.5	1.51	5.01	1.51	0.14	0.14
	48.5	1.51	5.01	1.51	0.14	0.14
Central point	96.6	3.01	10.0	3.01	0.14	0.13
	96.6	3.01	10.0	3.01	0.14	0.13
Axial point 25	193	3.01	10.0	3.01	0.14	0.13
	193	3.01	10.0	3.01	0.13	0.14
Axial point 28	96.6	3.01	0.01	3.01	0.12	0.14
	96.6	3.01	0.01	3.01	0.13	0.14

Four points from the design matrix (Table S1) were selected to conduct Sb(V)-SAWC sorption experiments. Sb,control = Sb concentrations recorded in the control experiments without SAWC; Sb,SAWC = Sb concentrations recorded in the SAWC suspensions at the end of sorption experiments. No Sb(V) sorption by SAWC was observed.

6. Miscellaneous results from aqueous phase measurements

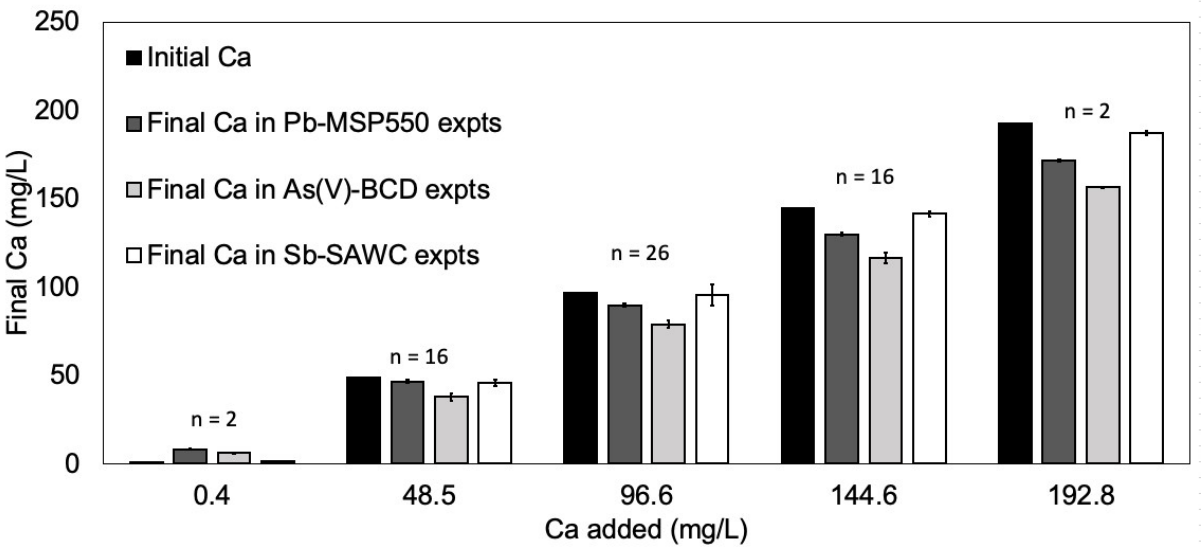

Figure S5. Aqueous phase Ca^{2+} concentrations at the end of all sorption experiments. The averaged values across different initial Ca^{2+} concentrations for each metal(loid)-BC are shown. Error bars represent the standard deviation of the values. "n" is the total number of tested water matrices at each initial Ca^{2+} concentration.

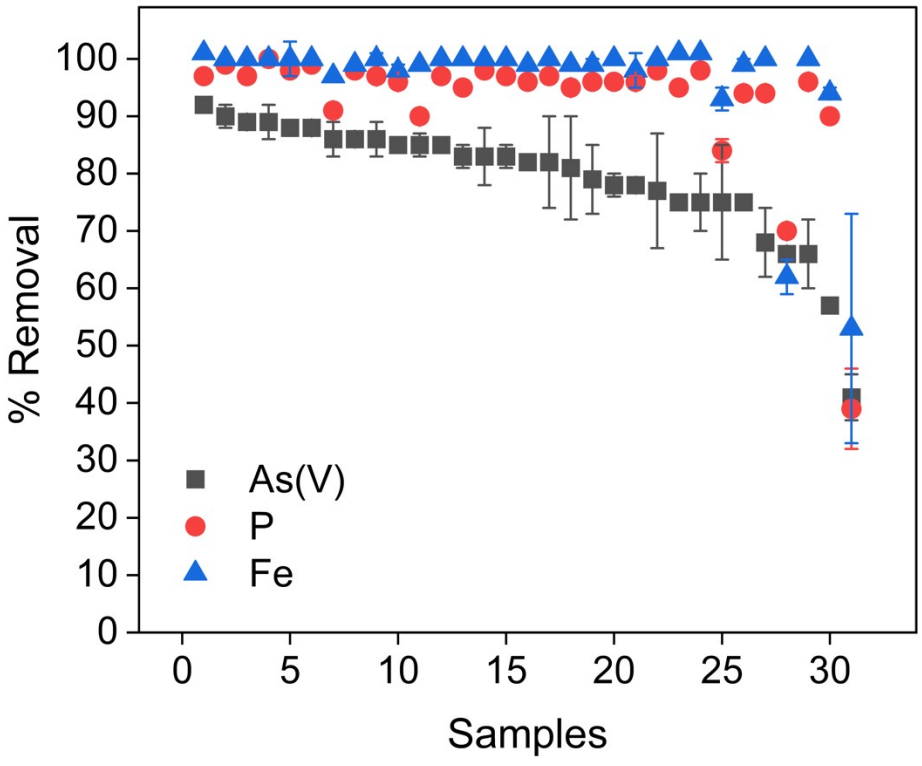

Figure S6. Removal of As(V), P, and total Fe across samples in As(V)-BCD experiments

7. Characterization of BCs and solid phase analysis

The specific surface area and pore volume of the washed pristine BCs was determined by N_2 physisorption isotherms at 77K based on the Brunauer, Emmett, and Teller (BET) theory after degassing at 105°C overnight (Quantachrome Nova 2000 analyzer, Quantachrome Instruments, USA) (Sigmund et al., 2017). The C, H, N, and S contents of the BCs were measured on an elemental analyzer (Elementar, Elementar Analysensysteme GmbH, Germany), and the sample was burned at 750°C for 6 hours to determine the ash content (ASTM D 1762-84, 2011). The O content was determined by difference: O% = 100 – (C + H + N + S + ash). A multiphase carbon analyzer (LECO RC612, LECO, USA) was used to quantify the total organic carbon (T<550°C) and the total inorganic carbon (50<T<1000°C) of the biochar-dolomite blend BC (BCD). Electron spin resonance spectroscopy (X-band Bruker Elexsys-II E500 ESR spectrometer, Bruker Biospin GmbH) was used to measure persistent free radicals in the solid BCs following a methodology detailed elsewhere (Sigmund et al., 2021). X-ray diffractograms of powdered samples were obtained using powder XRD (MiniFlex 600, Rigaku, Japan) equipped with a monochromator and a Cu Kα radiation source (λ = 1.54 Å) operating between 15.0 kV to 40 kV. Diffraction patterns were collected over a scan range of 2θ range of 10 to 70° (step size: 0.05° 2θ; scan speed: 10° min^{-1}) using a zero-background silicon base holder. For the BC showing presence of peaks, clearer (noise-reduced) diffractograms were obtained over a longer duration (step size: 0.05° 2θ; scan speed: 0.5° min^{-1}). The International Center for Diffraction Database (ICDD) was used to determine mineral phases. Scanning electron microscope (SEM) images of each pristine BC was obtained using a Zeiss Supra 55 VP (ZEISS Microscopy, Germany) scanning electron microscope (w.d.: 9.5 mm; magnification: 100X to 5000X; secondary electron voltage: 5 kV). Energy dispersive spectra were obtained from an Oxford X-Max^N 20 energy dispersive X-ray spectrometer attached to the SEM. An accelerating voltage of 20 kV was used. The EDS spectra were analyzed using the AZtecEnergy EDS software. Micro X-ray fluorescence (μXRF) imaging with a fine focused and high intensity beam (10 μm spot size) using a Horiba XGT 7000 (Horiba Ltd, Japan) was used for determining spatial distribution of Ca, P, and Fe on the BCs at the end of experiments at axial points of the CCD. For μXRF elemental mapping, the BCs were mixed with Hoechst wax C

micropowder as a binding agent (50:50 for SAWC, and 70:30 for MSP550 and BCD) to form 13 mm flat surfaced pellets.

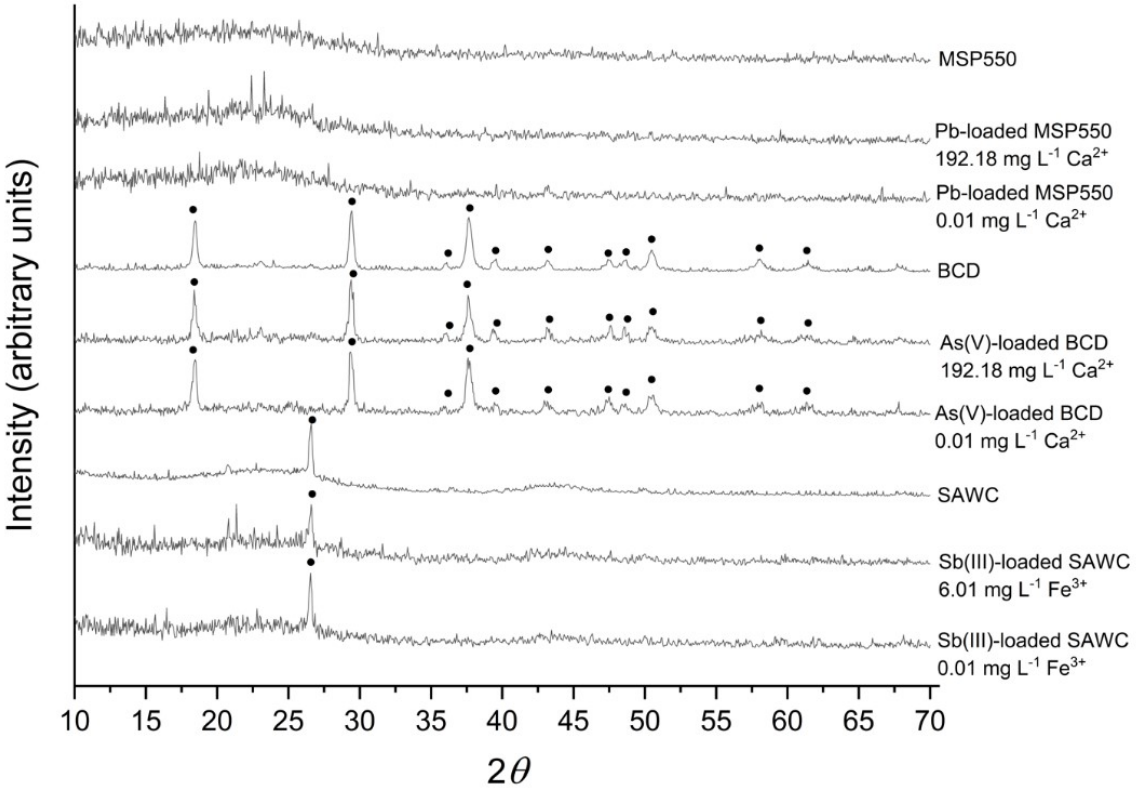

Figure S7. X-ray diffractograms of the BCs, both pristine as well after sorption experiments conducted using background solutions at selected end most axial points.

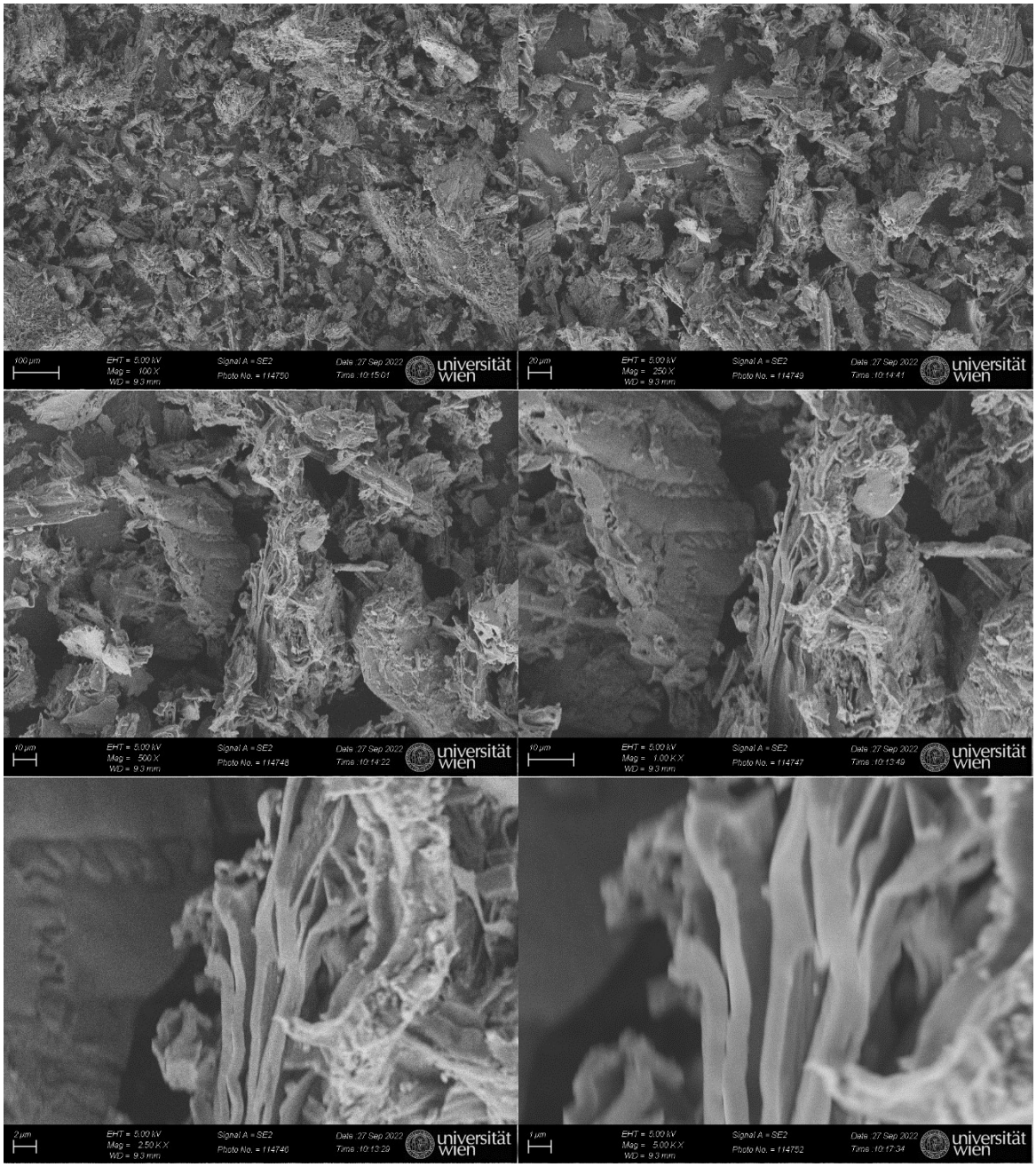

Figure S8. Scanning electron microscope images of MSP550 (w.d. 9.3 mm; EHT 5 kV; magnification from 100× to 5000×)

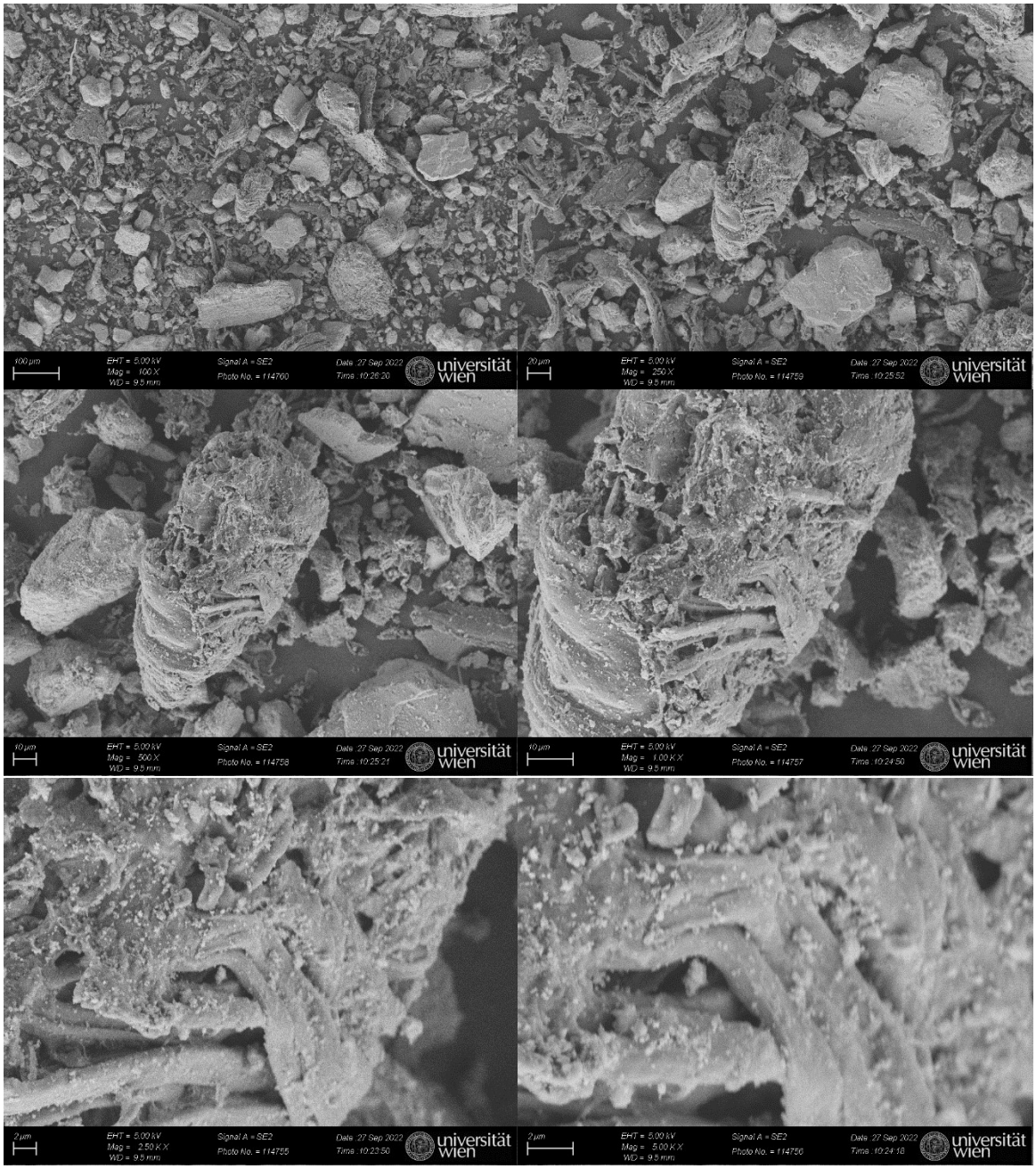

Figure S9. Scanning electron microscope images of BCD (w.d. 9.5 mm; EHT 5 kV; magnification from 100× to 5000×)

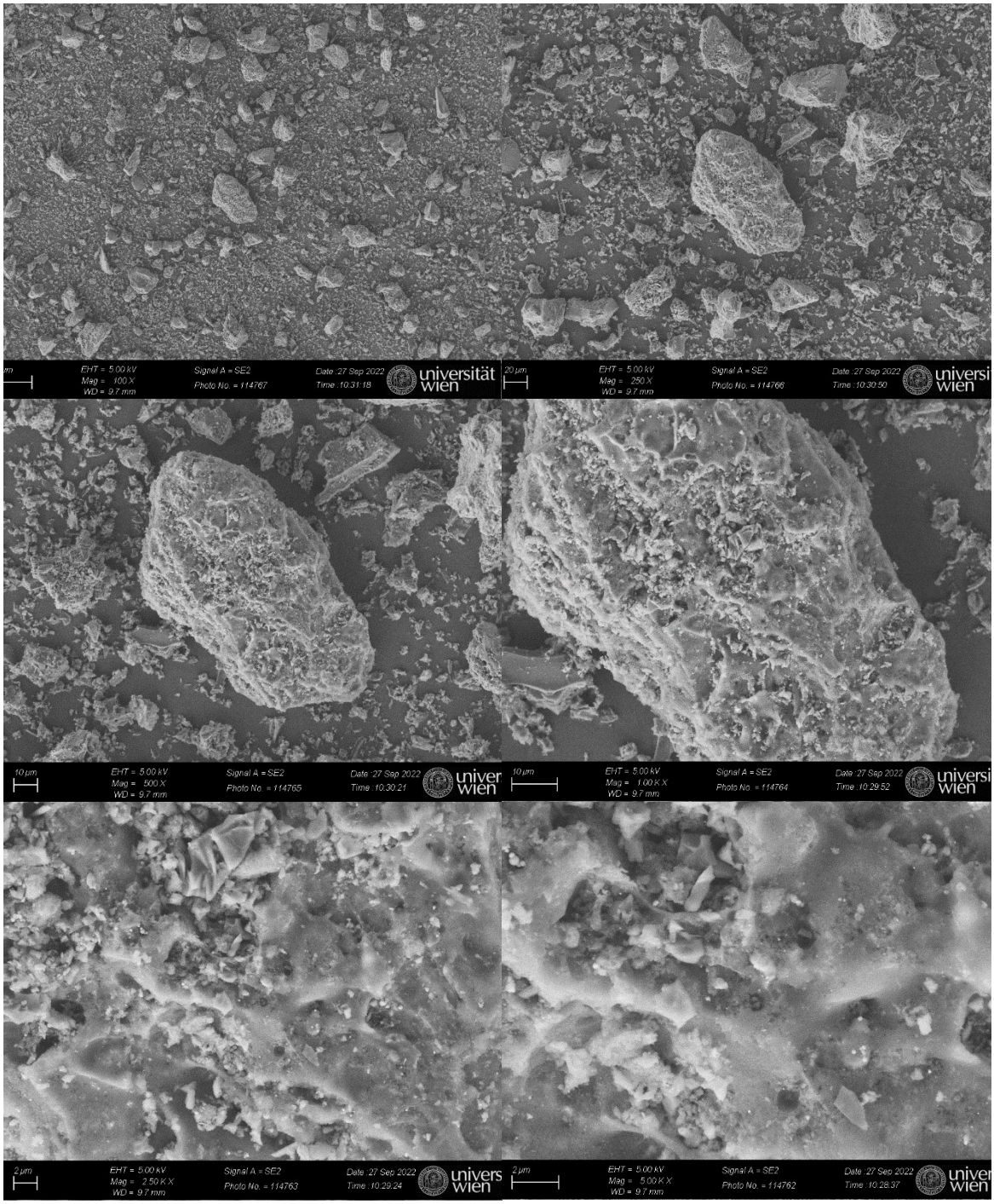

Figure S10. Scanning electron microscope images of SAWC (w.d. 9.7 mm; EHT 5 kV; magnification from 100× to 5000×)

(a)

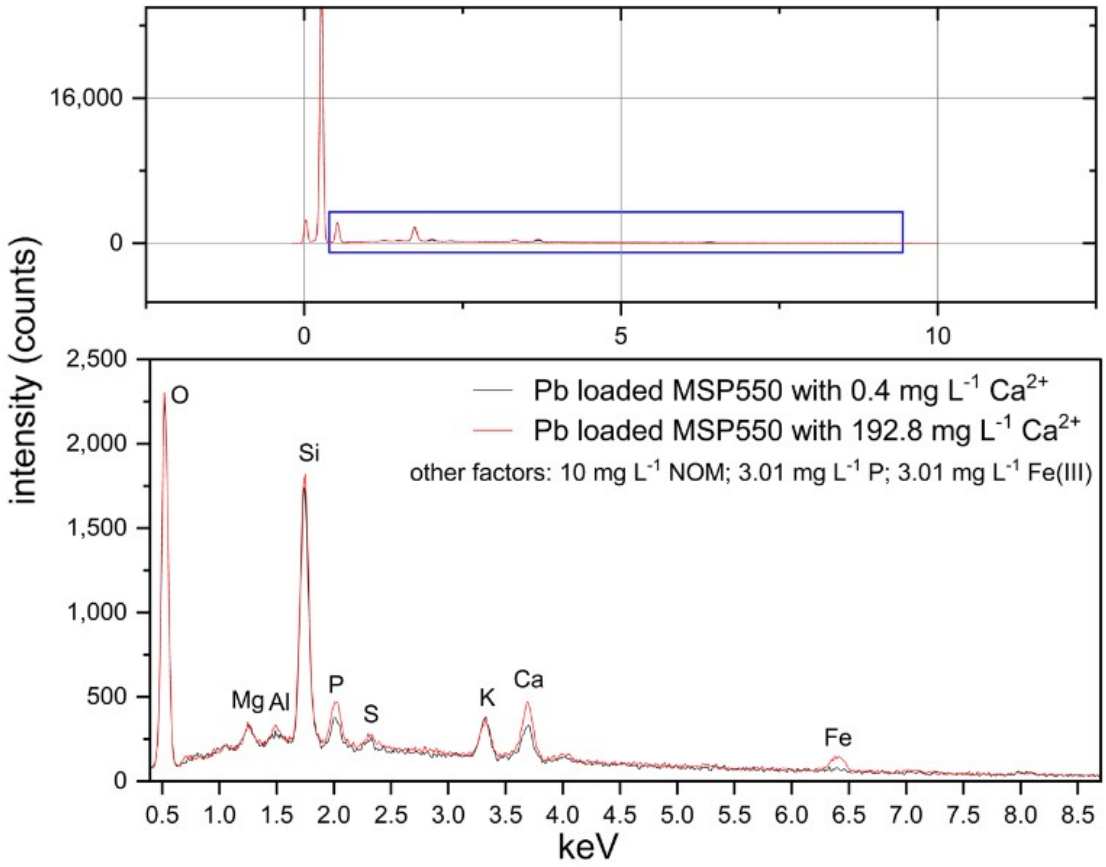
16,000
0
0
5
10
intensity (counts)
2,500
2,000
1,500
1,000
500
0
O
Si
Mg Al
P
S
K
Ca
Fe
Pb loaded MSP550 with 0.4 mg L-1 Ca2+
Pb loaded MSP550 with 192.8 mg L-1 Ca2+
other factors: 10 mg L-1 NOM; 3.01 mg L-1 P; 3.01 mg L-1 Fe(III)
0.5 1.0 1.5 2.0 2.5 3.0 3.5 4.0 4.5 5.0 5.5 6.0 6.5 7.0 7.5 8.0 8.5
keV

183

(b)

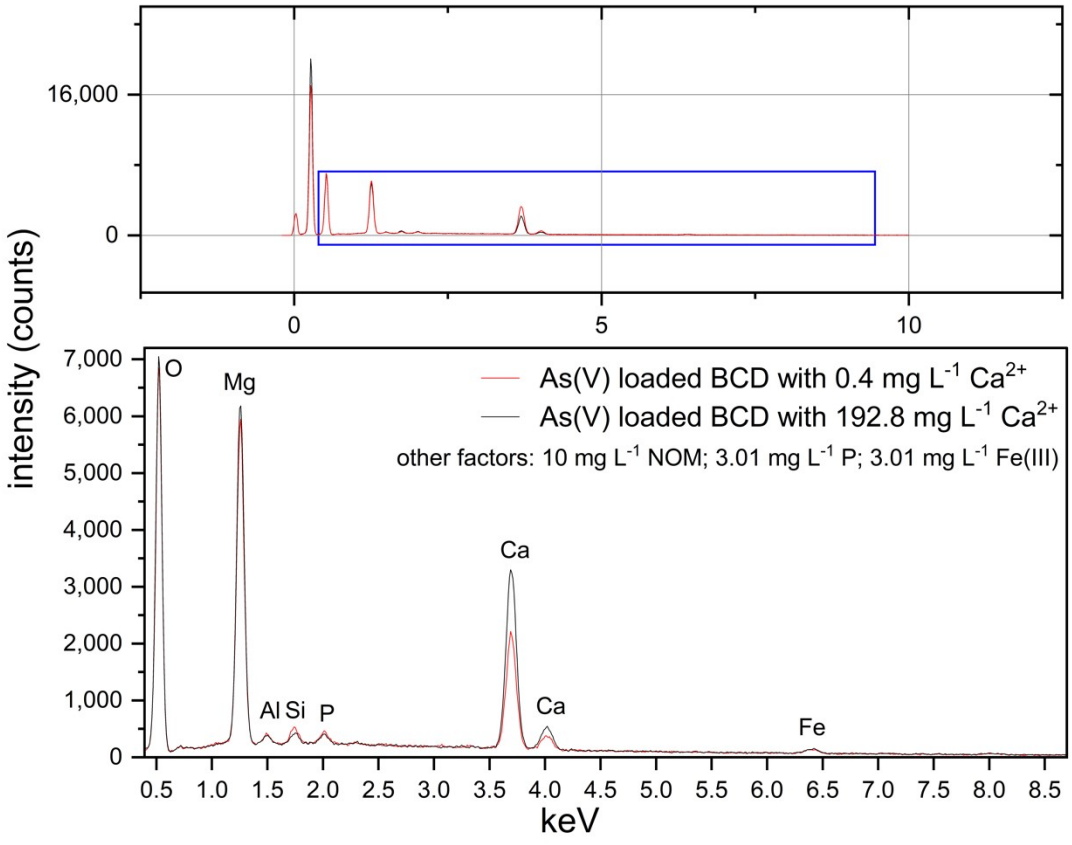
16,000
0
0
5
10
intensity (counts)
7,000
6,000
5,000
4,000
3,000
2,000
1,000
0
O
Mg
Al Si P
Ca
Ca
Fe
As(V) loaded BCD with 0.4 mg L-1 Ca2+
As(V) loaded BCD with 192.8 mg L-1 Ca2+
other factors: 10 mg L-1 NOM; 3.01 mg L-1 P; 3.01 mg L-1 Fe(III)
0.5 1.0 1.5 2.0 2.5 3.0 3.5 4.0 4.5 5.0 5.5 6.0 6.5 7.0 7.5 8.0 8.5
keV

184

(c)

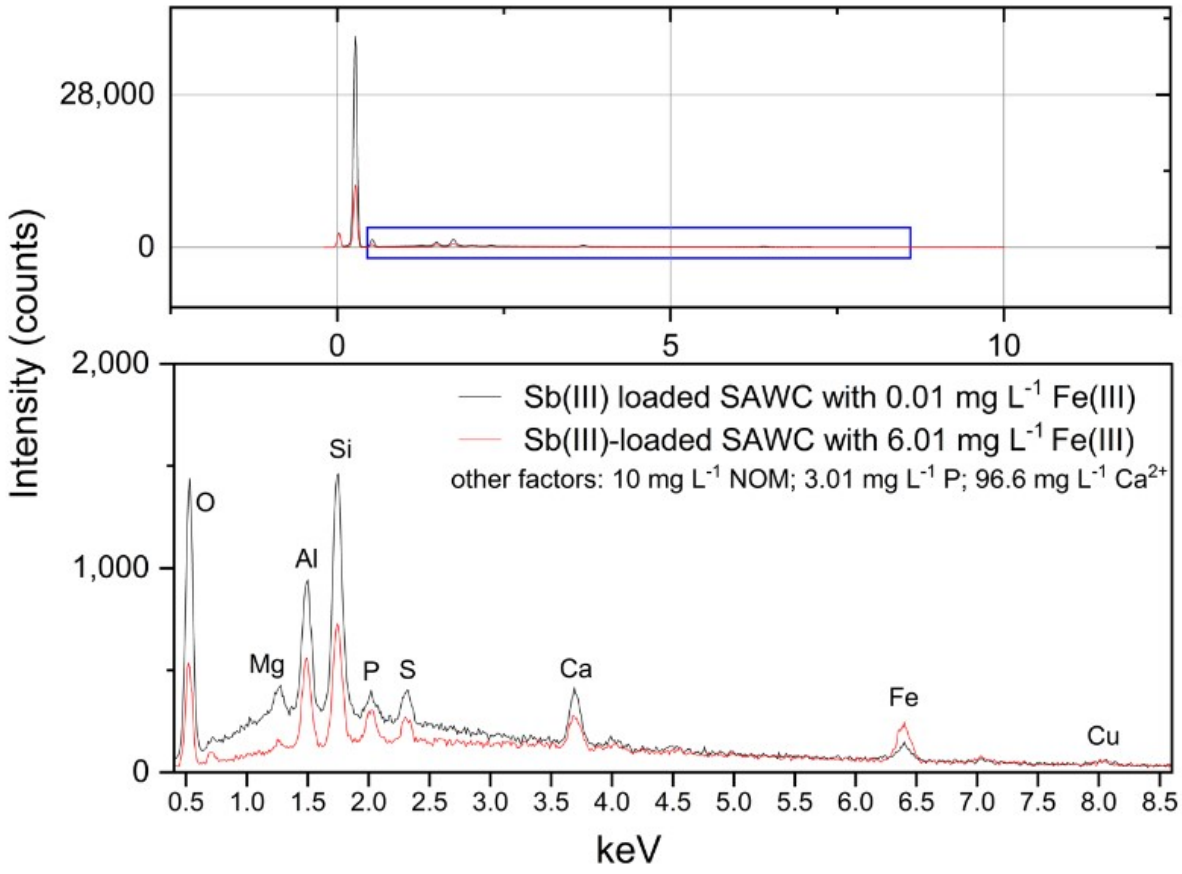

185

186 **Figure S11.** Energy dispersive spectra of the BCs after sorption experiments,
187 conducted using background solutions at selected end most axial points. (a) Pb-
188 MSP550; (b) As(V)-BCD; (c) Sb(III)-SAWC

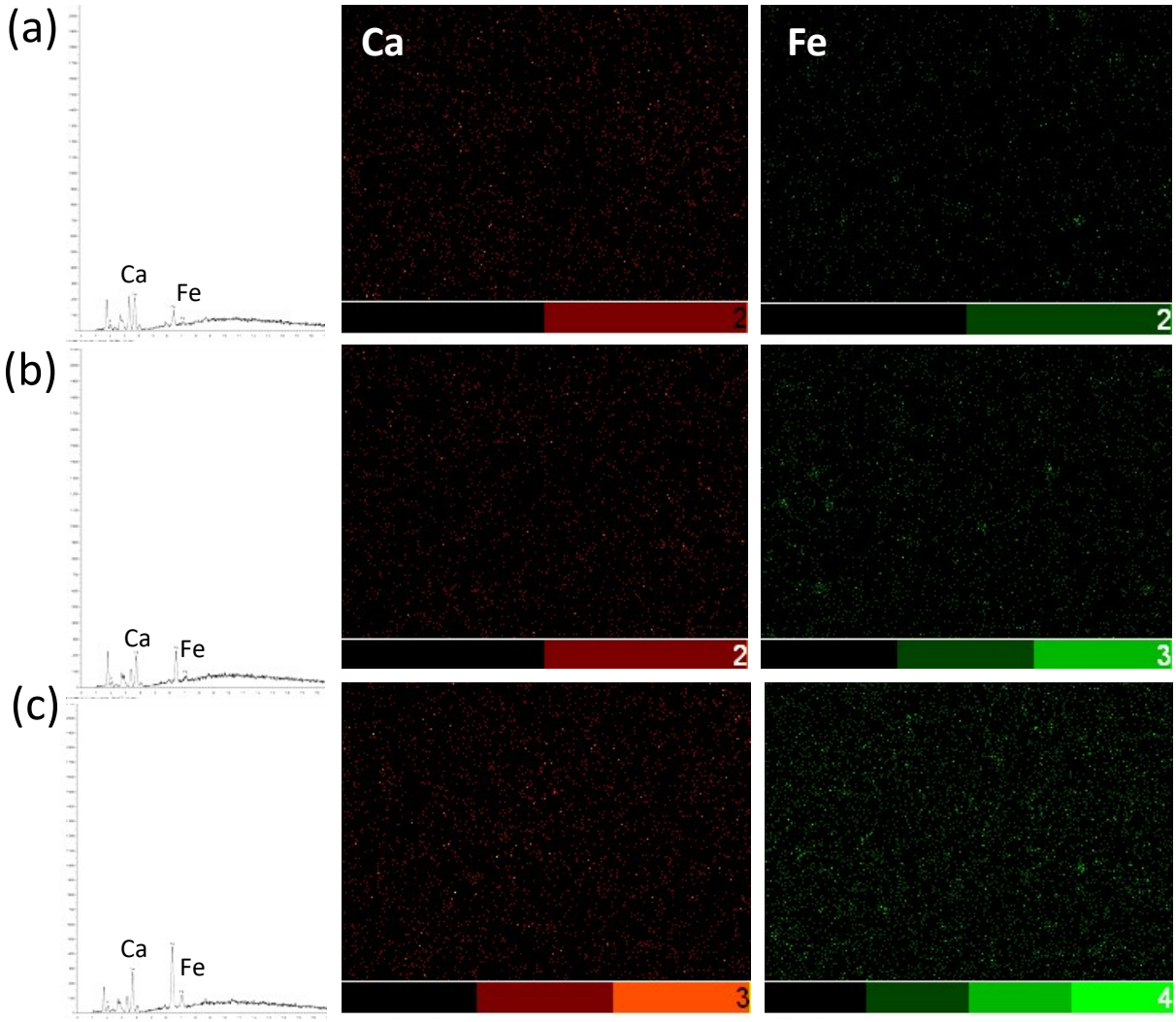

Figure S12. μ-XRF spectra and elemental maps (10 μm spot size) of Ca and Fe for **(a)** pristine MSP550; **(b)** MSP550 at the end of Pb sorption experiments for end most axial point 0.4 mg L^{-1} Ca^{2+} with other factors at "medium" level; **(c)** MSP550 at the end of As(V) sorption experiments for end most axial point 192.8 mg L^{-1} Ca^{2+} with other factors at "medium" level. Medium level: 3.01 mg L^{-1} Fe(III), 3.01 mg L^{-1} P, and 10 mg L^{-1} DOC as NOM.

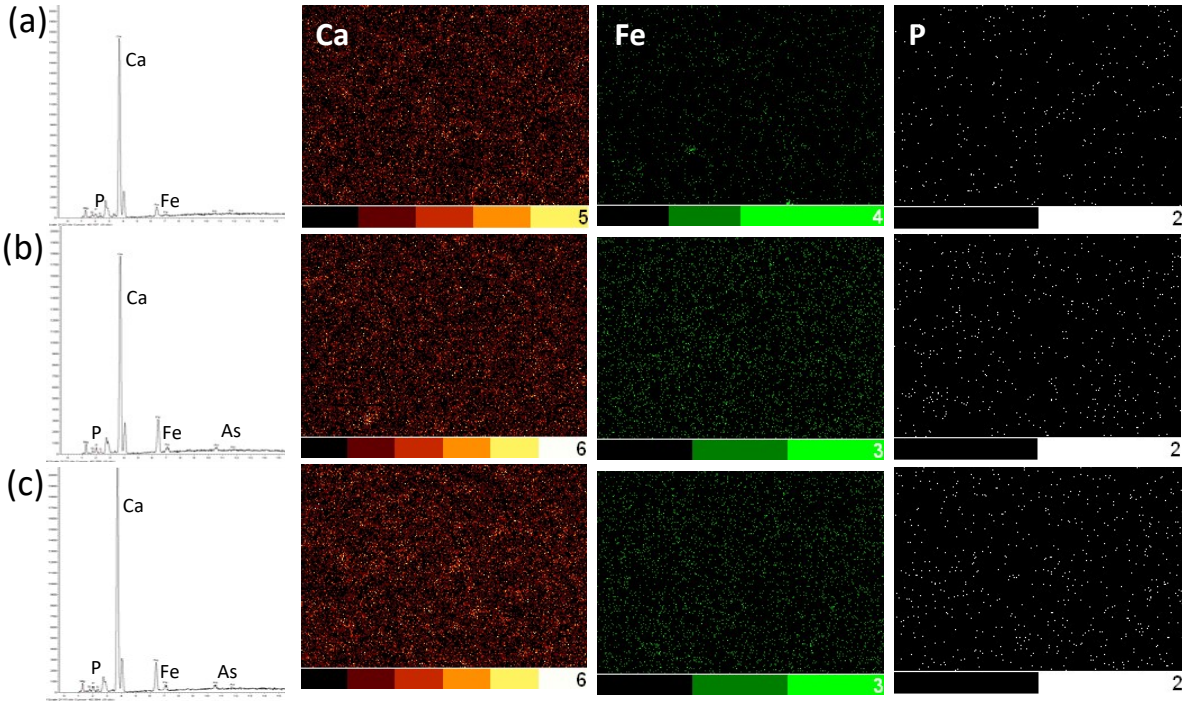

Figure S13. μ-XRF spectra and elemental maps (10 μm spot size) of Ca, Fe, and P for **(a)** pristine BCD; **(b)** BCD at the end of As(V) sorption experiments for end most axial point 0.4 mg L^{-1} Ca^{2+} with other factors at "medium" level; **(c)** BCD at the end of As(V) sorption experiments for end most axial point 192.8 mg L^{-1} Ca^{2+} with other factors at "medium" level. Medium level: 3.01 mg L^{-1} Fe(III), 3.01 mg L^{-1} P, and 10 mg L^{-1} DOC as NOM.

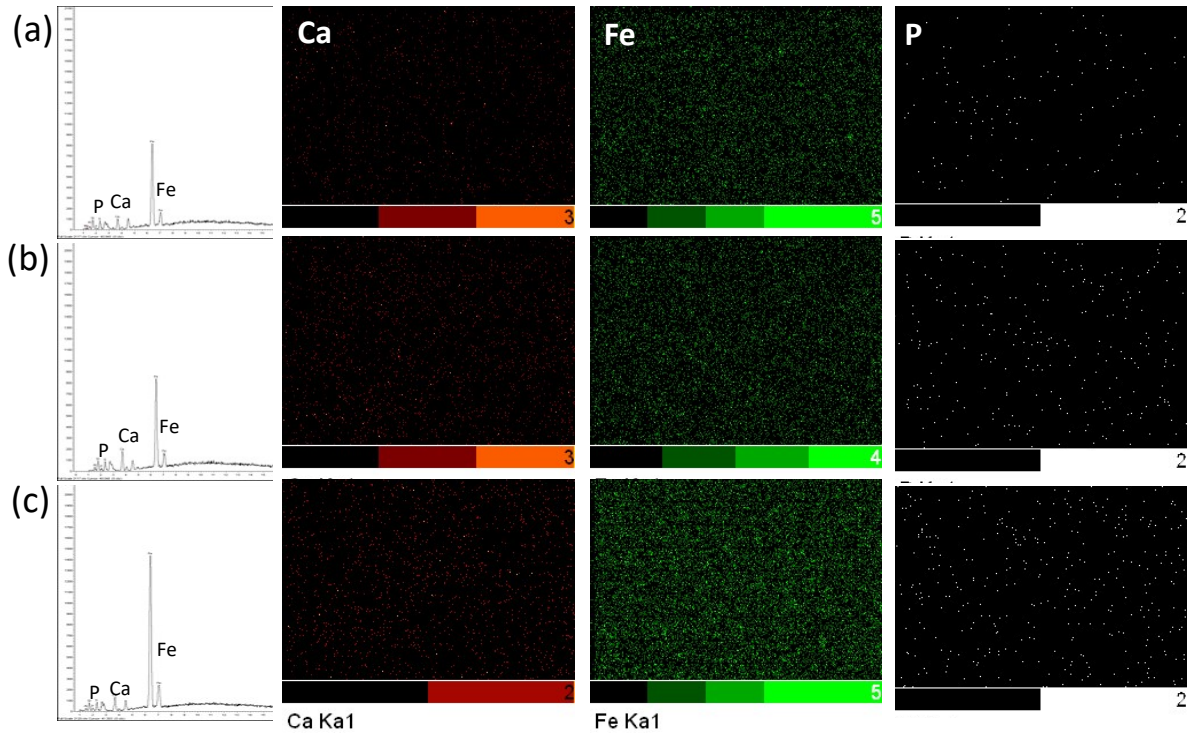

Figure S14. μ-XRF spectra and elemental maps (10 μm spot size) of Ca, Fe, and P for **(a)** pristine SAWC; **(b)** SAWC at the end of Sb(III) sorption experiments for endmost axial point 0.01 mg L^{-1} Fe(III) with other factors at "medium" level; **(c)** SAWC at the end of Sb(III) sorption experiments for end most axial point 6.01 mg L^{-1} Fe(III) with other factors at "medium" level. Medium level: 96.6 mg L^{-1} Ca^{2+}, 3.01 mg L^{-1} P, and 10 mg L^{-1} DOC as NOM.

References

ASTM D 1762-84, 2011. Standard Test Method for Chemical Analysis of Wood Charcoal., in: ASTM International. pp. 1–2. https://doi.org/10.1520/D1762-84R21

Sigmund, G., Hüffer, T., Hofmann, T., Kah, M., 2017. Biochar total surface area and total pore volume determined by N2 and CO2 physisorption are strongly influenced by degassing temperature. Science of the Total Environment 580, 770–775. https://doi.org/10.1016/j.scitotenv.2016.12.023

Sigmund, G., Santín, C., Pignitter, M., Tepe, N., Doerr, S.H., Hofmann, T., 2021. Environmentally persistent free radicals are ubiquitous in wildfire charcoals and remain stable for years. Communications Earth & Environment 2, 1–6. https://doi.org/10.1038/s43247-021-00138-2

Zheng, J., Iijima, A., Furuta, N., 2001. Complexation effect of antimony compounds with citric acid and its application to the speciation of antimony(iii) and antimony(v) using HPLC-ICP-MS. Journal of Analytical Atomic Spectrometry 16, 812–818. https://doi.org/10.1039/b101943k